Hindawi
Journal of Mathematics
Volume 2023, Article ID 9950023, 16 pages
https://doi.org/10.1155/2023/9950023

Research Article

On the Expected Discounted Penalty Function Using Physics-Informed Neural Network

Jiayu Wang[1] **and Houchun Wang**[2]

[1]*School of Mathematics, Hefei University of Technology, Hefei 230601, China*
[2]*School of Mathematics & Physics, Anhui Jianzhu University, Hefei 230601, China*

Correspondence should be addressed to Houchun Wang; wanghouchun7023@126.com

Received 3 July 2023; Revised 26 November 2023; Accepted 14 December 2023; Published 28 December 2023

Academic Editor: Barbara Martinucci

We study the expected discounted penalty at ruin under a stochastic discount rate for the compound Poisson risk model with a threshold dividend strategy. The discount rate is modeled by a Poisson process and a standard Brownian motion. By applying the differentiation method and total expectation formula, we obtain an integrodifferential equation for the expected discounted penalty function. From this integrodifferential equation, a renewal equation and an asymptotic formula satisfied by the expected discounted penalty function are derived. In order to solve the integrodifferential equation, we use a physics-informed neural network (PINN) for the first time in risk theory and obtain the numerical solutions of the expected discounted penalty function in some special cases of the penalty at ruin.

1. Introduction

For the first time in actuarial science, Gerber and Shiu [1] introduced the expected discounted penalty function which is also referred to as the Gerber–Shiu function. Since the seminal paper by [1], the Gerber–Shiu function has been widely studied and has become one of the most representative research directions in risk theory (see [2–4]). For the Gerber–Shiu function, the main goal is to consider three important random variables once at a time, namely, the time of ruin, the surplus immediately before ruin, and the deficit at ruin. Usually, the Gerber–Shiu function is used to evaluate the overall financial performance of an insurance company before going bankrupt. The special issue in volume 46, 2010, of the journal Insurance: Mathematics and Economics contains a selection of papers focused on the Gerber–Shiu function, with many further references therein. The expected discounted penalty function has attracted the interest of many actuaries since its inception. Ramsden and Papaioannou [5] considered a Markov-modulated risk model and derived an integrodifferential equation for the expected discounted penalty function, the asymptotic behavior of which was investigated in terms of Laplace transforms. Under a Lévy insurance risk process, the joint Laplace transform of ruin-time and ruin-position was presented by [6], and this Laplace transform can be used to compute the expected discounted penalty function via Laplace inversion. Preischl and Thonhauser [7] minimized expected discounted penalty functions in a Cramér–Lundberg model by choosing optimal reinsurance, showed the existence and uniqueness of the solution found by this method, and provided numerical examples involving light- and heavy-tailed claims. Martin–González and Kolkovska [8] studied a generalization of the expected discounted penalty function for a class of two-sided jump Lévy processes having positive jumps with a rational Laplace transform and provided an explicit expression for the generalized function in terms of functions depending only on the parameters of the Lévy process. The expected discounted penalty function provides a unified framework for the evaluation of various risk quantities. For a systematic study of the Gerber–Shiu theory, one can refer to references [1–3, 7–12].

In recent years, with the rapid advancement of artificial intelligence and machine learning theory, a number of

papers have focused on the numerical solution of differential equations and proposed novel learning machines to solve the differential equations (see [13–22]). Zhou et al. [13] constructed a neural network model, in which trigonometric function served as the activation function, added the initial condition of the integrodifferential equation satisfied by the ruin probability to the solver model, and obtained the numerical solutions to it. Ma et al. [14, 15] proposed an initial condition extreme learning machine and a novel structure automatic-determined Fourier extreme learning machine to realize numerical solutions of the partial differential equations, respectively. In particular, Raissi et al. [16] introduced physics-informed neural network (PINN), which was trained to solve supervised learning tasks while respecting any given laws of physics described by general nonlinear partial differential equations, and solved the problem of data-driven solutions to partial differential equations. Wu et al. [19] proposed a new physics-informed neural network (PINN) for solving the Hausdorff derivative Poisson equations on irregular domains by using the concept of Hausdorff fractal derivative and transformed the numerical solution of the partial differential equation into an optimization problem including governing equation and boundary conditions. In Zhang et al. [20], a novel deep learning technique, called multidomain physics-informed neural network (MDPINN), was presented to solve forward and inverse problems of steady-state heat conduction in multilayer media. Zhang et al. [21] numerically resolved linear and nonlinear transient heat conduction problems in multilayer composite materials using multidomain physics-informed neural networks. Compared to other existing approaches, the PINN is simple, straightforward, and easy-to-program, and it has been successfully applied in different fields recently. Numerical experiments indicate that the PINN methodology is accurate and effective, which provides a new idea for solving certain differential equations (see [16, 19–22]).

Although the expected discounted penalty function was proposed more than two decades ago and continues to play an important role in actuarial science research, there are still many unsolved problems such as the two here for generalizing the discount rate in this function from a constant to a random variable for the nonclassical risk model and looking for an effective numerical scheme for this function with no explicit solution (see [3, 5–12]).

The main goal of this paper is to partially address both of the above issues. The rest of this paper is organized as follows: In the latter part of the introduction section, the risk model of interest with a threshold dividend strategy is introduced together with the expected discounted penalty function with a random discount factor. The important technical analysis is carried out in Section 2, where the integrodifferential equation for the expected discounted penalty function is ultimately derived. In Section 3, in the case of a relatively large initial surplus, we obtain a renewal equation and, further, an asymptotic formula for the expected discounted penalty function. In Section 4, we give basic information about the structure of the neural network, the way the neural network is trained, and other basic details of the physics-informed neural network methodology to find numerical solutions of the integrodifferential equation in Section 2, and, by numerical examples, illustrate the effectiveness of the physics-informed neural network method.

In the classical compound Poisson risk model, the insurance company is assumed to collect premiums at a constant rate $c > 0$, whereas claims arrive successively according to the times of a Poisson process, henceforth denoted by $\{N_t; t \geq 0\}$ with Poisson parameter $\lambda > 0$. These successive individual claim amounts denoted by $\{X_1, X_2, \cdots\}$, independent of $\{N_t; t \geq 0\}$, are independent and identically distributed (i.i.d.) positive random variables with a common cumulative distribution function (c.d.f.) $F(x)$ that has a positive finite mean μ and a continuous probability density function $f(x) = F'(x)$. Consequently, the i.i.d. interclaim time random variables $\{T_1, T_2, \cdots\}$, independent of $\{X_1, X_2, \cdots\}$, have an exponential distribution with mean $1/\lambda$. The aggregate claims process is defined by $\left\{S_t = \sum_{i=1}^{N_t} X_i; t \geq 0\right\}$, where $S_t = 0$ if $N_t = 0$. Thus, the insurer's surplus process $\{U_t; t \geq 0\}$ is given by $U_t = u + ct - S_t$, where $u = U_0 \geq 0$ is the initial surplus. For more on the classical compound Poisson risk model, see [23, 24] which serve as encyclopedic references for all matters concerning ruin theory.

We now enrich the classical model. We assume that the insurance company is a stock company, and dividends are paid to the shareholders according to a threshold dividend strategy. Let $b > 0$ denote the constant barrier level, and $c_1 > 0$ be the annual premium rate if the surplus U_t is below the barrier level b. Let c^*, $0 < c^* \leq c_1$, be the annual dividend rate, i.e., when the insurer's surplus is above the barrier b, dividends are paid at rate c^*. Thus, the net premium rate after dividend payments is $c_2 = c_1 - c^*$. As usual, we assume the security loading condition, that is, the condition $c_2 - \lambda\mu > 0$ is fulfilled. Under such a strategy, the surplus process $\{U_t; t \geq 0\}$ can be expressed as follows:

$$U_t = \begin{cases} u + c_1 t - S_t, & 0 \leq U_t \leq b, \\ u + c_2 t - S_t, & U_t > b. \end{cases} \tag{1}$$

See [25, 26] and references therein for this type of risk model with threshold dividend strategy, and Figure 1 shows a graphical representation of a sample path of the surplus process.

Define the time of ruin as $T = \inf\{t | U_t < 0\}$, where $T = \infty$ if $U_t \geq 0$ for all $0 \leq t < \infty$. Then, U_{T-} denotes the surplus immediately before ruin and $|U_T|$ denotes the deficit at ruin. Let $w(x_1, x_2), 0 < x_1, x_2 < \infty$, be a bivariate nonnegative function which satisfies some mild integrable conditions. We now introduce the expected discounted penalty function

$$m(u) = \mathrm{E}\left[e^{-R_T} w\left(U_{T-}, \left|U_T\right|\right) I(T < \infty) | U_0 = u\right], \quad u \geq 0, \tag{2}$$

where $I(A)$ is the indicator function of an event A and $R_t, t \geq 0$, is interpreted as the accumulated interest force function. We assume that $R_t = \delta t + \alpha P_t + \beta B_t$, where δ, α, β all are the nonnegative constants, $\{P_t; t \geq 0\}$ is a Poisson process with Poisson parameter $\lambda^* > 0$, $\{B_t; t \geq 0\}$ is a standard Brownian motion, and $\{P_t; t \geq 0\}$, $\{B_t; t \geq 0\}$, and

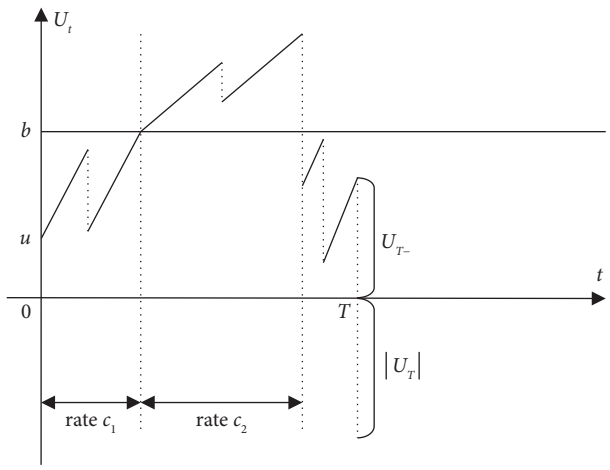

FIGURE 1: A graphical representation of a sample path of the surplus process.

$\{U_t; t \geq 0\}$ are assumed to be mutually independent (see [27, 28]). Since stochastic fluctuation of interest cannot be large in reality, and for simplicity, we might as well assume that $\delta \geq \lambda^* (e^{-\alpha} - 1) + \beta^2/2$.

In the setting of surplus processes without dividend strategy, [28–30] and the references therein generalized the known results on the expected discounted penalty function with constant discount rate in [1]. Li et al. [30] provided the first systematic numerical study on, via the popular Fourier-cosine method, finite-time expected discounted penalty functions with the risk process being driven by a generic Lévy subordinator.

The expected discounted penalty function $m(u)$ is a function of the initial surplus $U_0 = u \geq 0$. Many recent research studies on ruin-related quantities can be rooted to the expected discounted penalty function with constant discount rate, i.e., $R_T = \delta T$. For example, by setting $w(x_1, x_2) \equiv 1$ and $\delta = 0$, the expected discounted penalty function $m(u)$ reduces to the ruin probability as follows:

$$\phi(u) = \mathrm{E}\left[I(T < \infty) | U_0 = u\right] = \Pr\left[T < \infty | U_0 = u\right]. \quad (3)$$

Particularly, the first-step analysis for the expected discounted penalty function was adopted in [1] to derive a defective renewal equation, from which explicit solutions could be obtained. In the classical compound Poisson risk model without dividend strategy, Gerber and Shiu [1] gave the integrodifferential equation, the renewal equation, and the asymptotic formula for the expected discounted penalty function in the setting that $\delta \geq 0, \alpha = 0, \beta = 0$, i.e., $R_t = \delta t$, and Wang and Ling [28] gave these results in the setting that $\delta \geq 0, \alpha \geq 0, \beta \geq 0$, i.e., $R_t = \delta t + \alpha P_t + \beta B_t$. In this paper, we derive the integrodifferential equation and the renewal equation for the expected discounted penalty function $m(u)$ of (2) under the risk model (1) with a threshold dividend strategy and a random discount factor e^{-R_t}, where $R_t = \delta t + \alpha P_t + \beta B_t$, $\delta \geq 0, \alpha \geq 0, \beta \geq 0$, and also give a remark on the asymptotic. In order to efficiently obtain numerical results, physics-informed neural network (PINN) is used to give the numerical solutions of the expected discounted penalty function in some special cases of the penalty at ruin for the first time in risk theory.

2. Integrodifferential Equation for the Expected Discounted Penalty Function

In this section, we derive an integrodifferential equation for the expected discounted penalty function $m(u)$ by utilizing the strong Markov property of the Poisson process at claim instants.

Clearly, the expected discounted penalty function $m(u)$ behaves differently, depending on whether the initial surplus u is below or above the barrier level b. Hence, we write

$$m(u) = \begin{cases} m_1(u), & 0 \leq u \leq b, \\ m_2(u), & u > b. \end{cases} \quad (4)$$

Proposition 1. *The expected discounted penalty function $m(u)$ satisfies the following integrodifferential equation for $0 \leq u < \infty$:*

$$m_1'(u) = \frac{\lambda + \delta - \lambda^* (e^{-\alpha} - 1) - \beta^2/2}{c_1} m_1(u) - \frac{\lambda}{c_1} \int_0^u m_1(u - x) f(x) \mathrm{d}x - \frac{\lambda}{c_1} \int_u^\infty w(u, x - u) f(x) \mathrm{d}x, \quad 0 \leq u \leq b, \quad (5)$$

$$m_2'(u) = \frac{\lambda + \delta - \lambda^* (e^{-\alpha} - 1) - \beta^2/2}{c_2} m_2(u) - \frac{\lambda}{c_2} \int_0^u m(u - x) f(x) \mathrm{d}x - \frac{\lambda}{c_2} \int_u^\infty w(u, x - u) f(x) \mathrm{d}x, \quad u > b, \quad (6)$$

where

$$\int_0^u m(u-x)f(x)\mathrm{d}x = \int_0^{u-b} m_2(u-x)f(x)\mathrm{d}x + \int_{u-b}^u m_1(u-x)f(x)\mathrm{d}x, \quad u > b. \tag{7}$$

Proof. For $0 \le u \le b$, we condition on the time T_1 and the amount X_1 of the first claim. Contingent on this time T_1 of the first claim, there are two options: the first claim occurs before the time $t_0 = (b-u)/c_1$ when the surplus has attained the barrier level, i.e., $u + c_1 t_0 = b$ or it occurs after attaining the barrier. When we consider the amount X_1 of the first claim, there are two possibilities as well: after it, the surplus process $\{U_t; t \ge 0\}$ starts all over again with new initial surplus or the first claim leads to ruin.

It needs to distinguish between two cases. First, $0 \le T_1 \le t_0 = (b-u)/c_1$ and the surplus has not yet reached the barrier b. In this case, the surplus immediately before the time T_1 is $u + c_1 T_1$. Second, $T_1 > t_0 = (b-u)/c_1$ that is no claim occurs before the surplus exceeds the barrier b. In this case, the surplus immediately before time T_1 is $U_{T_1} = b + c_2(T_1 - t_0)$ and there are three possibilities at time T_1 for the amount X_1 of the first claim, that is more than $U_{T_1} = b + c_2(T_1 - t_0)$, less than $U_{T_1} - b = c_2(T_1 - t_0)$, or between $U_{T_1} - b$ and U_{T_1}.

In view of the strong Markov property of the surplus process $\{U_t; t \ge 0\}$ at claim instants and total expectation formula, for $0 \le u \le b$, we obtain

$$\begin{aligned} m(u) = m_1(u) = {} & \int_0^{t_0} \mathrm{E}\left[e^{-R_t}\right]\left(\int_0^{u+c_1 t} m_1(u + c_1 t - x)\mathrm{d}F(x) + \int_{u+c_1 t}^{\infty} w(u + c_1 t, x - u - c_1 t)\mathrm{d}F(x)\right)\lambda e^{-\lambda t}\mathrm{d}t \\ & + \int_{t_0}^{\infty} \mathrm{E}\left[e^{-R_t}\right]\left(\int_0^{c_2(t-t_0)} m_2(b + c_2(t-t_0) - x)\mathrm{d}F(x)\right)\lambda e^{-\lambda t}\mathrm{d}t \\ & + \int_{t_0}^{\infty} \mathrm{E}\left[e^{-R_t}\right]\left(\int_{c_2(t-t_0)}^{b+c_2(t-t_0)} m_1(b + c_2(t-t_0) - x)\mathrm{d}F(x)\right)\lambda e^{-\lambda t}\mathrm{d}t \\ & + \int_{t_0}^{\infty} \mathrm{E}\left[e^{-R_t}\right]\left(\int_{b+c_2(t-t_0)}^{\infty} w(b + c_2(t-t_0), x - b - c_2(t-t_0))\mathrm{d}F(x)\right)\lambda e^{-\lambda t}\mathrm{d}t, \end{aligned} \tag{8}$$

where

$$t_0 = \frac{b-u}{c_1}, \qquad \mathrm{E}\left[e^{-R_t}\right] = e^{-\delta t}\mathrm{E}\left[e^{-\alpha P_t}\right]\mathrm{E}\left[e^{-\beta B_t}\right] = e^{-\delta t} e^{\lambda^* t(e^{-\alpha}-1)} e^{\beta^2 t/2}. \tag{9}$$

Letting $k(t) = e^{-(\lambda+\delta-\lambda^*(e^{-\alpha}-1)-\beta^2/2)t}$ leads to

$$\begin{aligned} m_1(u) = {} & \lambda \int_0^{t_0} k(t)\left(\int_0^{u+c_1 t} m(u + c_1 t - x)\mathrm{d}F(x) + \int_{u+c_1 t}^{\infty} w(u + c_1 t, x - u - c_1 t)\mathrm{d}F(x)\right)\mathrm{d}t \\ & + \lambda \int_{t_0}^{\infty} k(t)\left(\int_0^{b+c_2(t-t_0)} m(b + c_2(t-t_0) - x)\mathrm{d}F(x)\right)\mathrm{d}t \\ & + \lambda \int_{t_0}^{\infty} k(t)\left(\int_{b+c_2(t-t_0)}^{\infty} w(b + c_2(t-t_0), x - b - c_2(t-t_0))\mathrm{d}F(x)\right)\mathrm{d}t. \end{aligned} \tag{10}$$

We then get

$$m_1(u) = \lambda \int_0^{t_0} k(t)\left(g\left(u + c_1 t\right) + h\left(u + c_1 t\right)\right)\mathrm{d}t + \lambda \int_{t_0}^{\infty} k(t)\left(g\left(b + c_2\left(t - t_0\right)\right) + h\left(b + c_2\left(t - t_0\right)\right)\right)\mathrm{d}t, \quad 0 \le u \le b, \tag{11}$$

where

$$g(y) = \int_0^y m(y - x) f(x)\mathrm{d}x, \qquad h(y) = \int_y^{\infty} w(y, x - y) f(x)\mathrm{d}x, \tag{12}$$

where $h(y)$ is a function which is independent of b and $m(u)$.

We write the constant number $\lambda + \delta - \lambda^*\ (e^{-\alpha} - 1) - \beta^2/2$ as τ. Changing variables in (11) by $s = u + c_1 t$ and $s = b + c_2(t - t_0)$ results in

$$m_1(u) = \frac{\lambda}{c_1} e^{\tau u/c_1} \int_u^b e^{-\tau s/c_1}\left(g(s) + h(s)\right)\mathrm{d}s + \frac{\lambda}{c_2} e^{\tau u/c_1} \int_b^{\infty} e^{-\tau\left(s/c_2 - b/c_2 + b/c_1\right)}\left(g(s) + h(s)\right)\mathrm{d}s, \quad 0 \le u \le b. \tag{13}$$

By differentiating both sides of the equation (13) with respect to u, we obtain

$$m_1'(u) = \frac{\lambda\tau}{c_1^2} e^{\tau u/c_1} \int_u^b e^{-\tau s/c_1}\left(g(s) + h(s)\right)\mathrm{d}s - \frac{\lambda}{c_1}\left(g(u) + h(u)\right) + \frac{\lambda\tau}{c_1 c_2} e^{\tau u/c_1} \int_b^{\infty} e^{-\tau\left(s/c_2 - b/c_2 + b/c_1\right)}\left(g(s) + h(s)\right)\mathrm{d}s = \frac{\lambda + \delta - \lambda^*\left(e^{-\alpha} - 1\right) - \beta^2/2}{c_1} m_1(u) - \frac{\lambda}{c_1} g(u) - \frac{\lambda}{c_1} h(u), \quad 0 \le u \le b. \tag{14}$$

So, equation (5) is correct.

For $u > b$, the surplus immediately before time T_1 of the first claim is $U_{T_1} = u + c_2 T_1$, and at time T_1, the surplus may be less than 0, more than b, or between 0 and b. In the same way as deriving (5), it is obvious that

$$\begin{aligned} m(u) = m_2(u) &= \int_0^{\infty} \mathrm{E}\left[e^{-R_t}\right]\left(\int_0^{u + c_2 t - b} m_2\left(u + c_2 t - x\right)\mathrm{d}F(x)\right)\lambda e^{-\lambda t}\mathrm{d}t \\ &+ \int_0^{\infty} \mathrm{E}\left[e^{-R_t}\right]\left(\int_{u + c_2 t - b}^{u + c_2 t} m_1\left(u + c_2 t - x\right)\mathrm{d}F(x)\right)\lambda e^{-\lambda t}\mathrm{d}t \\ &+ \int_0^{\infty} \mathrm{E}\left[e^{-R_t}\right]\left(\int_{u + c_2 t}^{\infty} w\left(u + c_2 t, x - u - c_2 t\right)\mathrm{d}F(x)\right)\lambda e^{-\lambda t}\mathrm{d}t \\ &= \lambda \int_0^{\infty} e^{-\left(\lambda + \delta - \lambda^*\left(e^{-\alpha} - 1\right) - \beta^2/2\right)t}\left(\int_0^{u + c_2 t - b} m_2\left(u + c_2 t - x\right)\mathrm{d}F(x)\right)\mathrm{d}t \\ &+ \lambda \int_0^{\infty} e^{-\left(\lambda + \delta - \lambda^*\left(e^{-\alpha} - 1\right) - \beta^2/2\right)t}\left(\int_{u + c_2 t - b}^{u + c_2 t} m_1\left(u + c_2 t - x\right)\mathrm{d}F(x)\right)\mathrm{d}t \\ &+ \lambda \int_0^{\infty} e^{-\left(\lambda + \delta - \lambda^*\left(e^{-\alpha} - 1\right) - \beta^2/2\right)t}\left(\int_{u + c_2 t}^{\infty} w\left(u + c_2 t, x - u - c_2 t\right)\mathrm{d}F(x)\right)\mathrm{d}t, \quad u > b. \end{aligned} \tag{15}$$

We then get

$$m_2(u) = \lambda \int_0^\infty e^{-\left(\lambda+\delta-\lambda^*\left(e^{-\alpha}-1\right)-\beta^2/2\right)t} \left(g\left(u+c_2t\right)+h\left(u+c_2t\right)\right)\mathrm{d}t, \quad u>b, \tag{16}$$

where

$$\begin{aligned} g(y) &= \int_0^y m(y-x)f(x)\mathrm{d}x, \\ h(y) &= \int_y^\infty w(y,x-y)f(x)\mathrm{d}x. \end{aligned} \tag{17}$$

Note that $\tau = \lambda + \delta - \lambda^*(e^{-\alpha}-1) - \beta^2/2$. Substituting $u + c_2t$ with s in (16) yields

$$m_2(u) = \frac{\lambda}{c_2} e^{\tau u/c_2} \int_u^\infty e^{-\tau s/c_2}(g(s)+h(s))\mathrm{d}s, \quad u>b, \tag{18}$$

and then differentiating both sides of the equation (18) with respect to u yields the integrodifferential equation (6).

$$\begin{aligned} m_2'(u) &= \frac{\lambda+\delta-\lambda^*\left(e^{-\alpha}-1\right)-\beta^2/2}{c_2} m_2(u) \\ &\quad - \frac{\lambda}{c_2} g(u) - \frac{\lambda}{c_2} h(u), \quad u>b, \end{aligned} \tag{19}$$

where

$$\begin{aligned} g(u) &= \int_0^u m(u-x)f(x)\mathrm{d}x = \int_0^{u-b} m_2(u-x)f(x)\mathrm{d}x \\ &\quad + \int_{u-b}^u m_1(u-x)f(x)\mathrm{d}x, \quad u>b, \end{aligned} \tag{20}$$

by which the proof is concluded. □

2.1. Remarks

(1) The integrodifferential equation (5) for $m_1(u)$ does not involve $m_2(u)$ but the integrodifferential equation (6) for $m_2(u)$ incorporates $m_1(u)$.

(2) Equations (13) and (18) show that $m(u)$ is continuous, and especially, for $u = b$, $m_1(b) = m_2(b+)$, i.e., $m_1(b) = \lim_{u\longrightarrow b^+} m_2(u)$.

(3) We examine $m'(u)$ when $u = b$. However, the same is not true for $m'(u)$ at $u = b$. To see this, let $u \longrightarrow b^+$ in (6) and employ the integrodifferential form of $m_1(u)$ in (5) afterwards. We then have

$$\begin{aligned} m_2'(b+) &= \lim_{u\longrightarrow b^+} m_2'(u) = \frac{\lambda+\delta-\lambda^*\left(e^{-\alpha}-1\right)-\beta^2/2}{c_2} m_2(b+) - \frac{\lambda}{c_2}\int_0^b m_1(b-x)f(x)\mathrm{d}x - \frac{\lambda}{c_2}h(b) \\ &= \frac{\lambda+\delta-\lambda^*\left(e^{-\alpha}-1\right)-\beta^2/2}{c_2} m_1(b) + \frac{c_1}{c_2}\left(m_1'(b-) - \frac{\lambda+\delta-\lambda^*\left(e^{-\alpha}-1\right)-\beta^2/2}{c_1} m_1(b)\right). \end{aligned} \tag{21}$$

This results in $c_1 m_1'(b-) = c_2 m_2'(b+)$, where $m_1'(b-)$ is a left-derivative and $m_2'(b+)$ is a right-derivative. Thus, the expected discounted penalty function $m(u)$ at $u = b$ is continuous but not differentiable.

3. Renewal Equation for the Expected Discounted Penalty Function

In this section, we first obtain a renewal equation for $m_2(u)$, $u > b$. Finally, the asymptotic formula for $m(u)$ is derived by virtue of this renewal equation.

Let

$$\begin{aligned} m_\rho(u) &= e^{-\rho u} m(u), \\ m_{\rho,1}(u) &= e^{-\rho u} m_1(u), \\ m_{\rho,2}(u) &= e^{-\rho u} m_2(u), \end{aligned} \tag{22}$$

where ρ is the unique nonnegative solution to the Lundberg equation of ξ:

$$-c_2\xi + \lambda + \delta - \lambda^*\left(e^{-\alpha}-1\right) - \frac{\beta^2}{2} = \lambda \int_0^\infty e^{-\xi x} f(x)\mathrm{d}x. \tag{23}$$

From

$$\begin{aligned} \frac{d}{\mathrm{d}\xi}\int_0^\infty e^{-\xi x} f(x)\mathrm{d}x &= -\int_0^\infty e^{-\xi x} x f(x)\mathrm{d}x < 0, \\ \frac{d^2}{\mathrm{d}\xi^2}\int_0^\infty e^{-\xi x} f(x)\mathrm{d}x &= \int_0^\infty e^{-\xi x} x^2 f(x)\mathrm{d}x > 0, \end{aligned} \tag{24}$$

it is clear that equation (23) has a unique nonnegative root and a unique negative root which are denoted as $\rho \geq 0$ and $-R < 0$, respectively, because of $\delta \geq \lambda^*(e^{-\alpha}-1) + \beta^2/2$. See [28] and Figure 2 for the solutions to equation (23) which will be used later on.

Proposition 2. *The expected discounted penalty function $m_2(u)$ satisfies the following renewal equation for $u > b$:*

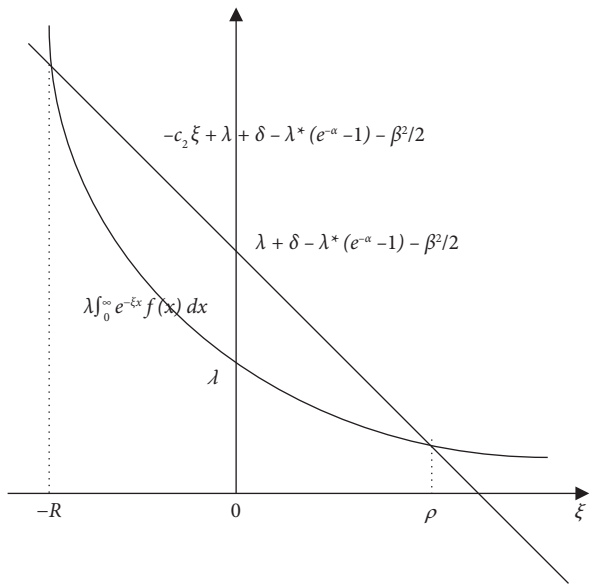

Figure 2: The two roots of equation (23).

$$c_2 m_2(u) = \lambda \int_0^b \left(\int_{u-y}^\infty e^{\rho(u-x-y)} f(x)\mathrm{d}x \right) m_1(y)\mathrm{d}y + \lambda \int_b^u \left(\int_{u-y}^\infty e^{\rho(u-x-y)} f(x)\mathrm{d}x \right) m_2(y)\mathrm{d}y + \lambda \int_u^\infty e^{\rho(u-x)} h(x)\mathrm{d}x, \tag{25}$$

where $h(x) = \int_x^\infty w(x, y-x) f(y)\mathrm{d}y$.

Proof. For $u > b$, multiplying both sides of (6) with $e^{-\rho u}$ and applying the product rule for differentiation, we get

$$c_2 m_{\rho,2}'(u) = \left(-c_2\rho + \lambda + \delta - \lambda^*\left(e^{-\alpha} - 1\right) - \frac{\beta^2}{2} \right) m_{\rho,2}(u) - \lambda \int_0^{u-b} m_{\rho,2}(u-x) e^{-\rho x} f(x)\mathrm{d}x - \lambda \int_{u-b}^u m_{\rho,1}(u-x) e^{-\rho x} f(x)\mathrm{d}x - \lambda e^{-\rho u} h(u), \tag{26}$$

where $h(u) = \int_u^\infty w(u, x-u) f(x)\mathrm{d}x$.

By (23), then equation (26) reduces to

$$\begin{aligned} \frac{c_2}{\lambda} m_{\rho,2}'(u) &= m_{\rho,2}(u) \int_0^\infty e^{-\rho x} f(x)\mathrm{d}x - \int_0^{u-b} m_{\rho,2}(u-x) e^{-\rho x} f(x)\mathrm{d}x \\ &\quad - \int_{u-b}^u m_{\rho,1}(u-x) e^{-\rho x} f(x)\mathrm{d}x - e^{-\rho u} h(u) \\ &= m_{\rho,2}(u) \int_0^\infty e^{-\rho x} f(x)\mathrm{d}x - \int_b^u m_{\rho,2}(x) e^{-\rho(u-x)} f(u-x)\mathrm{d}x \\ &\quad - \int_0^b m_{\rho,1}(x) e^{-\rho(u-x)} f(u-x)\mathrm{d}x - e^{-\rho u} h(u). \end{aligned} \tag{27}$$

For $s \geq b$, we integrate both sides of the equation (27) from $u = b$ to $u = s$, and then have

$$\begin{aligned}\frac{c_2}{\lambda}\left(m_{\rho,2}(s)-m_{\rho,2}(b)\right)&=\int_b^s\left(\int_0^\infty e^{-\rho x}f(x)\mathrm{d}x\right)m_{\rho,2}(u)\mathrm{d}u-\int_b^s\left(\int_b^u m_{\rho,2}(x)e^{-\rho(u-x)}f(u-x)\mathrm{d}x\right)\mathrm{d}u\\&\quad-\int_b^s\left(\int_0^b m_{\rho,1}(x)e^{-\rho(u-x)}f(u-x)\mathrm{d}x\right)\mathrm{d}u-\int_b^s e^{-\rho u}h(u)\mathrm{d}u\\&=\int_b^s\left(\int_0^\infty e^{-\rho x}f(x)\mathrm{d}x\right)m_{\rho,2}(u)\mathrm{d}u-\int_b^s\left(\int_x^s e^{-\rho(u-x)}f(u-x)\mathrm{d}u\right)m_{\rho,2}(x)\mathrm{d}x\\&\quad-\int_0^b\left(\int_b^s e^{-\rho(u-x)}f(u-x)\mathrm{d}u\right)m_{\rho,1}(x)\mathrm{d}x-\int_b^s e^{-\rho u}h(u)\mathrm{d}u\\&=\int_b^s\left(\int_0^\infty e^{-\rho x}f(x)\mathrm{d}x\right)m_{\rho,2}(u)\mathrm{d}u-\int_b^s\left(\int_0^{s-u} e^{-\rho x}f(x)\mathrm{d}x\right)m_{\rho,2}(u)\mathrm{d}u\\&\quad-\int_0^b\left(\int_{b-u}^{s-u} e^{-\rho x}f(x)\mathrm{d}x\right)m_{\rho,1}(u)\mathrm{d}u-\int_b^s e^{-\rho u}h(u)\mathrm{d}u.\end{aligned}\tag{28}$$

It follows that

$$\begin{aligned}\frac{c_2}{\lambda}\left(m_{\rho,2}(s)-m_{\rho,2}(b)\right)&=\int_b^s\left(\int_{s-u}^\infty e^{-\rho x}f(x)\mathrm{d}x\right)m_{\rho,2}(u)\mathrm{d}u\\&\quad-\int_0^b\left(\int_{b-u}^{s-u} e^{-\rho x}f(x)\mathrm{d}x\right)m_{\rho,1}(u)\mathrm{d}u-\int_b^s e^{-\rho u}h(u)\mathrm{d}u.\end{aligned}\tag{29}$$

By letting $s\longrightarrow\infty$, the first term on both sides of (29) vanishes. Thus, we have

$$\begin{aligned}\frac{c_2}{\lambda}m_{\rho,2}(b)&=\int_0^b\left(\int_{b-u}^\infty e^{-\rho x}f(x)\mathrm{d}x\right)m_{\rho,1}(u)\mathrm{d}u\\&\quad+\int_b^\infty e^{-\rho u}h(u)\mathrm{d}u.\end{aligned}\tag{30}$$

By (29) and (30), we obtain

$$\begin{aligned}\frac{c_2}{\lambda}m_{\rho,2}(s)&=\int_b^s\left(\int_{s-u}^\infty e^{-\rho x}f(x)\mathrm{d}x\right)m_{\rho,2}(u)\mathrm{d}u\\&\quad+\int_0^b\left(\int_{s-u}^\infty e^{-\rho x}f(x)\mathrm{d}x\right)m_{\rho,1}(u)\mathrm{d}u\\&\quad+\int_s^\infty e^{-\rho u}h(u)\mathrm{d}u.\end{aligned}\tag{31}$$

Applying

$$\begin{aligned}m_{\rho,1}(s)&=e^{-\rho s}m_1(s),\\m_{\rho,2}(s)&=e^{-\rho s}m_2(s),\end{aligned}\tag{32}$$

and multiplying (31) with $e^{\rho s}$, it follows that

$$\begin{aligned}\frac{c_2}{\lambda}m_2(s)&=\int_b^s\left(\int_{s-u}^\infty e^{\rho(s-x-u)}f(x)\mathrm{d}x\right)m_\rho(u)\mathrm{d}u\\&\quad+\int_0^b\left(\int_{s-u}^\infty e^{\rho(s-x-u)}f(x)\mathrm{d}x\right)m_\rho(u)\mathrm{d}u\\&\quad+\int_s^\infty e^{\rho(s-u)}h(u)\mathrm{d}u.\end{aligned}\tag{33}$$

Changing variables in (33) yields

$$\begin{aligned}\frac{c_2}{\lambda}m_2(u)&=\int_b^u\left(\int_{u-y}^\infty e^{\rho(u-x-y)}f(x)\mathrm{d}x\right)m_2(y)\mathrm{d}y\\&\quad+\int_0^b\left(\int_{u-y}^\infty e^{\rho(u-x-y)}f(x)\mathrm{d}x\right)m_1(y)\mathrm{d}y\\&\quad+\int_u^\infty e^{\rho(u-x)}h(x)\mathrm{d}x,\quad u>b,\end{aligned}\tag{34}$$

which is the required result. □

3.1. Remarks

(1) We know $m(u)$ consists of two parts: $m_1(u)$ and $m_2(u)$. To determine $m(u)$, we consider $m_1(u)$ which have been incorporated in equation (25) for $m_2(u)$. It is known from [4] that the general solution of $m_1(u)$ is of the following form:

$$m_1(u) = m_\infty(u) + \eta v(u), \quad 0 \le u \le b. \tag{35}$$

Here, η is an arbitrary constant to be determined; the function $m_\infty(u)$ is the expected discounted penalty function with no dividend strategy, that is, the expected discounted penalty function with barrier level ∞. As shown in [1, 28], the function $m_\infty(u)$ is the solution to the following renewal equation and its applications have been studied extensively,

$$c_1 m_\infty(u) = \lambda \int_0^u \left(\int_{u-y}^\infty e^{\rho(u-x-y)} f(x)\mathrm{d}x \right) m_\infty(y)\mathrm{d}y + \lambda \int_u^\infty e^{\rho(u-x)} h(x)\mathrm{d}x. \tag{36}$$

Here, $h(x) = \int_x^\infty w(x, y-x) f(y)\mathrm{d}y$.

The second function $v(u)$ is a nontrivial solution to the following homogeneous integrodifferential equation:

$$\begin{aligned} v'(u) &= \frac{\lambda + \delta - \lambda^* \left(e^{-\alpha} - 1\right) - \beta^2/2}{c_1} v(u) \\ &\quad - \frac{\lambda}{c_1} \int_0^u (u-x) f(x) v \mathrm{d}x, \end{aligned} \tag{37}$$

with initial condition defined (without loss of generality) to be $v(0) = 1$.

The constant η, which we specify by implementing equation (35) and returning to (25), satisfy

$$\begin{aligned} m_\infty(b) + \eta v(b) = m_1(b) &= \lim_{u \longrightarrow b^+} m_2(u) \\ &= \frac{\lambda}{c_2} \int_0^b \left(\int_{b-y}^\infty e^{\rho(b-x-y)} f(x)\mathrm{d}x \right) (m_\infty(y) + \eta v(y))\mathrm{d}y + \frac{\lambda}{c_2} \int_b^\infty e^{\rho(b-x)} h(x)\mathrm{d}x. \end{aligned} \tag{38}$$

Thus,

$$\eta = \frac{\lambda/c_2 \int_0^b \left(\int_{b-y}^\infty e^{\rho(b-x-y)} f(x)\mathrm{d}x \right) m_\infty(y)\mathrm{d}y + \lambda/c_2 \int_b^\infty e^{\rho(b-x)} h(x)\mathrm{d}x - m_\infty(b)}{v(b) - \lambda/c_2 \int_0^b \left(\int_{b-y}^\infty e^{\rho(b-x-y)} f(x)\mathrm{d}x \right) v(y)\mathrm{d}y}. \tag{39}$$

(2) Equation (25) may be restated as

$$\begin{aligned} c_2 m(u) &= \lambda \int_0^u \left(\int_{u-y}^\infty e^{\rho(u-x-y)} f(x)\mathrm{d}x \right) m(y)\mathrm{d}y \\ &\quad + \lambda \int_u^\infty e^{\rho(u-x)} h(x)\mathrm{d}x, u > b. \end{aligned} \tag{40}$$

Since equation (40) for $m_2(u)$ has the exact same form as equation (3.4) of [28], we may apply the same approach as far as [28] obtained the asymptotic formula (3.18) of [28], and then we have an asymptotic formula for the expected discounted penalty function $m(u)$

$$m(u) \sim \frac{\lambda \int_0^\infty \int_0^\infty \left(e^{Rx} - e^{-\rho x}\right) w(x, y) f(x+y)\mathrm{d}x\,\mathrm{d}y}{\lambda \int_0^\infty e^{Rx} x f(x)\mathrm{d}x - c_2} e^{-Ru}, \quad \text{for } u \longrightarrow \infty, \tag{41}$$

where ρ and $-R$ are the unique nonnegative root and the unique negative root of equation (23), respectively, and the notation $\varphi(u) \sim \psi(u)$, for $u \longrightarrow \infty$, means $\lim_{u\longrightarrow\infty}\varphi(u)/\psi(u) = 1$.

4. Numerical Results

In this section, we use the physics-informed neural network (PINN) method to find numerical solutions of the integrodifferential equation (5) for the expected discounted penalty function $m(u)$ in three special cases of the penalty at ruin (see [13–16, 19–21]). In addition, we also give asymptotic numerical solutions of (6) for $m(u)$ by the asymptotic formula (41).

4.1. Introduction to the Algorithm. Let us start by concentrating on the calculation of numerical solutions of the integrodifferential equation:

$$\lambda_0 m(u) + \lambda_1 m^{'}(u) + \lambda_2 m^{''}(u) = \int_0^u m(u-x) f(x)\mathrm{d}x + h(u), \quad u \geq 0, \tag{42}$$

where $m(u)$ denotes the hidden solution, $\lambda_0, \lambda_1, \lambda_2$ are the constants, and both of $f(x)$ and $h(u)$ are the nonnegative given functions.

The first integral on the right-hand side of (42) is the convolution $(m * f)(u)$. We assume that $m(u)$ satisfies the integrodifferential equation (42) with an initial and boundary condition of $m(u) = l(u)$, where $l(u)$ is a given function.

We define the function $g(u)$ as follows:

$$g(u) = \lambda_0 m(u) + \lambda_1 m^{'}(u) + \lambda_2 m^{''}(u) - (m * f)(u) - h(u), \quad u \geq 0. \tag{43}$$

Then, we chose to jointly approximate the latent function $m(u)$ and the convolution $(m * f)(u)$ by a M-layer fully-connected neural network with N neurons per layer, where the neural network takes u as an input and has two outputs. Let $\widehat{m}(u;\boldsymbol{\theta})$ and $(\widetilde{m} * f)(u;\boldsymbol{\theta})$ be the two outputs of the neural network that are used to approximate the real solution $m(u)$ of equation (42) and the convolution $(m * f)(u)$, respectively, where $\boldsymbol{\theta}$ is the random initialized parameter which represents the weights and biases of the neural network. This prior assumption along with equation (43) result in a physics-informed neural network (PINN) that takes u as an input and outputs $\widehat{g}(u;\boldsymbol{\theta})$ which is used to approximate $g(u)$ by (43). This network (PINN) can be derived by applying the automatic differentiation technique for the differentiating compositions of functions and by applying the output $(\widetilde{m} * f)(u;\boldsymbol{\theta})$ for the integral of functions and has the same parameters $\boldsymbol{\theta}$ as the fully-connected neural network representing $m(u)$ and $(m * f)(u)$, albeit with different activation functions due to the action of the integrodifferential operator. The shared parameters $\boldsymbol{\theta}$ between the two neural networks can be learned by minimizing the following mean squared error loss function.

The mean squared error loss function is defined as follows:

$$\text{Loss} = L_m + L_g, \tag{44}$$

where

$$\begin{aligned} L_m &= \frac{1}{N_m}\sum_{i=1}^{N_m}\left|\widehat{m}\left(u_m^i\right) - l^i\right|^2, \\ L_g &= \frac{1}{N_g}\sum_{i=1}^{N_g}\left|\widehat{g}\left(u_g^i\right)\right|^2 \\ &= \frac{1}{N_g}\sum_{i=1}^{N_g}\left|\lambda_0\widehat{m}\left(u_g^i\right) + \lambda_1\widehat{m}^{'}\left(u_g^i\right) + \lambda_2\widehat{m}^{''}\left(u_g^i\right) - (\widetilde{m} * f)\left(u_g^i\right) - h\left(u_g^i\right)\right|^2. \end{aligned} \tag{45}$$

Here, $\left\{u_g^i\right\}_{i=1}^{N_g}$ are the points in the interior of the computational domain for $g(u)$. $\{u_m^i, l^i\}_{i=1}^{N_m}$ denote the initial and boundary training data on $m(u)$ and account for both boundary and initial condition. Calculating L_g requires the derivatives $\widehat{m}^{'}(u), \widehat{m}^{''}(u)$ of the output $\widehat{m}(u)$ of the fully-connected neural network and the output $(\widetilde{m} * f)(u)$.

In the above PINN, an activation function should be employed to train the fully-connected neural network in order to find the relationship between the input and output. We use the hyperbolic tangent function $\tanh(x) = (e^x - e^{-x})/(e^x + e^{-x})$ as the activation function. The principle for this physics-informed neural network methodology is minimizing the loss function Loss by training the neural networks so that the output $\widehat{m}(u)$ of the fully-connected neural network approaches the real solution of the equation (42). Once the training is complete, extrapolation is performed and the numerical solution of equation (42) is obtained. The structure of the proposed PINN is illustrated in Figure 3, and the workflow of realizing a numerical solution of equation (42) using the PINN is as follows:

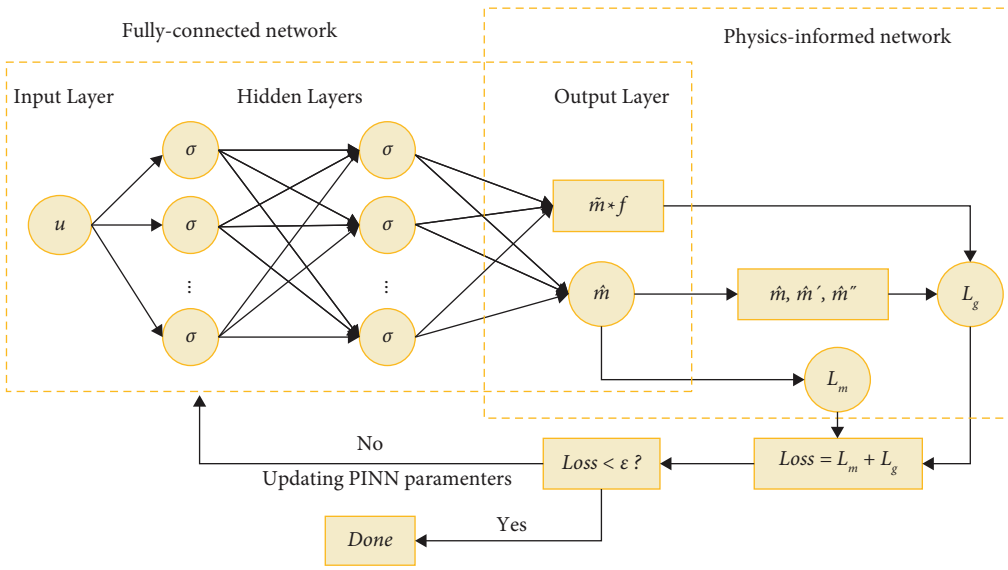

Figure 3: The PINN framework for solving the integrodifferential equation.

Step 1: Generate the initial and boundary training data on $m(u)$ and the collocation points in the interior of the computational domain for $g(u)$. The total number N_m of training data is relatively small (a few dozen up to a few hundred points).

Step 2: Specify the optimizer, the tolerance, the number of iterations.

Step 3: Construct a fully-connected neural network with random initialized parameters $\boldsymbol{\theta}$. The model trained consists of a series of fully connect operations with a $\tan h$ operation between each one. Specify the number M of fully connect operations and the number N of neurons for each fully connect operation. The first fully connect operation has an input channel corresponding to the input u. The last fully connect operation has two outputs $\widehat{m}(u;\boldsymbol{\theta})$ and $(\widetilde{m} * f)(u;\boldsymbol{\theta})$. Define the parameters for each of the operations. Initialize the parameters for the first fully connect operation, for each of the remaining intermediate fully connect operations, and for the final fully connect operation, respectively.

Step 4: Construct a physics-informed neural network $\widehat{g}(u;\boldsymbol{\theta})$ by substituting $\widehat{m}(u;\boldsymbol{\theta})$ and $(\widetilde{m} * f)(u;\boldsymbol{\theta})$ into the governing equation via automatic differentiation and arithmetic operations.

Step 5: Create the loss function Loss as shown in equation (44)

Step 6: Train the fully-connected neural network to find the best parameters $\boldsymbol{\theta}$ by minimizing the loss function Loss.

Step 7: Obtain the numerical solution by substituting the resultant parameters $\boldsymbol{\theta}$ into the neural network $\widehat{m}(u;\boldsymbol{\theta})$.

The rest of this section is organized as follows. In the rest of Section 4.1, we use a numerical example to demonstrate the effectiveness and accuracy of the proposed PINN method for obtaining the numerical solution of the integrodifferential equation. Section 4.2 presents two numerical examples of solving equations (5) and (6), respectively, where we again use the PINN method in the first numerical example. In particular, since the integrodifferential equations in these examples have only initial condition and no boundary condition, we assume that the boundary condition is $m(u) = e^{-u}$ for the PINN.

By conditional probability and total probability formula, Dickson [31] obtained that the ruin probability $\phi(u)$, in the Sparre Andersen risk model with a probability density function $k(t) = \lambda^2 t e^{-\lambda t}$ of the interclaim time, satisfies the integrodifferential equation along with initial condition which is given by

$$c^2\phi''(u) - 2\lambda c\phi'(u) + \lambda^2\phi(u) = \lambda^2\int_0^u \phi(u-t)f(t)\mathrm{d}t + \lambda^2[1-F(u)], \tag{46}$$

$$c^2 s_0\phi(0) = c^2 s_0 - 2\lambda c + \lambda^2\mu, \tag{47}$$

where $s_0 > 0$ is the solution of the algebraic equation

$$c^2s^2 - 2\lambda cs + \lambda^2 = \lambda^2 \int_0^{+\infty} e^{-sx} dF(x), \tag{48}$$

and $F(x)$ is the individual claim amount distribution function that has a positive finite mean μ. In the case of the exponential distribution $F(x) = 1 - e^{-\gamma x}$, by equations (46) and (47), Dickson [31] obtained an explicit solution of the ruin probability $\phi(u)$, which is expressed as follows:

$$\phi(u) = \frac{2\lambda^2 e^{2\lambda - c\gamma - \sqrt{(2\lambda - c\gamma)^2 + 8c\lambda\gamma - 4\lambda^2}/2cu}}{c^2\gamma^2 + 2c\lambda\gamma + c\gamma\sqrt{(2\lambda - c\gamma)^2 + 8c\lambda\gamma - 4\lambda^2}}, \quad u \geq 0. \tag{49}$$

We take advantage of the package MATLAB R2022b to examine the effectiveness and accuracy of the PINN method for obtaining the numerical solution of equation (46). Suppose $\lambda = 1, \gamma = 1, c = 1.5$. By (49), the exact solution of the ruin probability is $\phi(u) = 0.2092e^{-0.7908u}$. Given the computational domain [0,50] of u, we select 25 equal points to enforce the initial condition $\phi(0) = 0.2092$, select 25 equally spaced points to enforce the boundary condition $m(u) = e^{-u}$, and randomly select 10,000 points across the computational domain to enforce the outputs of the network to fulfill equation (46). This dataset is then used to train a 9-layer fully-connected neural network with 20 neurons and a hyperbolic tangent activation function per hidden layer by minimizing the mean square error loss function Loss of (44) using the L-BFGS optimizer (see [16]). Then, we obtain a numerical solution of equation (46) by the above PINN.

The change in the value of the loss function Loss is shown in Figure 4. Figure 5 displays the results of our experiment and shows a comparison between of the exact solution and the numerical solution of equation (46). Figure 6 and Table 1 give the errors of approximate solution obtained by using the PINN. The results show that the numerical solution is in good agreement with the exact solution when the initial surplus u takes on different values, in particular, when the initial surplus u is greater than 10.

4.2. Numerical Solutions of the Integrodifferential Equation

Example 1. Suppose $c_1 = 0.6, c_2 = 0.4, \lambda = 0.5, \delta = 0.06, \lambda^* = 0.125, \alpha = 0.01, \beta = 0.2$, and $f(x) = e^{-x}$. Solving equation (23) leads to $\rho = 0.7310$ and $-R = -0.2779$. We use the above PINN method to obtain the numerical solution of equation (5) for $m(u), 0 \leq u \leq b$, and then get the following results:

(1) Choose $w(x, y) \equiv 1$. For this case, the expected discounted penalty function

$$m(u) = E\left[e^{-(\delta T + \alpha P_T + \beta B_T)} I(T < \infty) | U_0 = u\right], \tag{50}$$

is the extension of the Laplace transform of the time of ruin. By equations (35)–(39), the initial condition of equation (5) is $m(0) = 0.7221$. The change in the loss function is shown in Figure 7(a), and the numerical solution of $m(u)$ is shown in Figure 8(a), respectively.

(2) Choose $w(x, y) = e^{0.01x}$. For this case, $m(0) = 0.7263$. The change in the loss function is shown in Figure 7(b), and the numerical solution of $m(u)$ is shown in Figure 8(b), respectively.

(3) Choose $w(x, y) = (1 - e^{1-y}) \vee 0$, which was interpreted as the payoff at exercise of a perpetual American put option by Gerber and Shiu [1]. For this case, $m(0) = 0.1328$. The change in the loss function is shown in Figure 7(c), and the numerical solution of $m(u)$ is shown in Figure 8(c), respectively.

Example 2. Suppose $c_2 = 0.4, \lambda = 0.5, \delta = 0.06, \lambda^* = 0.125, \alpha = 0.01, \beta = 0.2$ and the individual claim amount distribution is $\Gamma(a, \gamma)$ with density function

$$f(x) = F'(x) = \frac{\gamma^a e^{-\gamma x} x^{a-1}}{\Gamma(a)}, \quad x \geq 0, \tag{51}$$

where $a = \gamma = 0.01$ (see Chapter 1, Examples 18 and 19 of [24]).

Solving equation (23) leads to $\rho = 0.136193$ and $-R = -0.00999827$. These apply to the situation of Proposition 1. Hence,

$$\begin{aligned} m(u) = {} & 0.0120055 \int_0^u \left(\int_{u-y}^{\infty} e^{-0.146193x} x^{-0.99} dx \right) e^{0.136193(u-y)} m(y) dy \\ & + 0.0120055 \int_u^{\infty} \left(\int_y^{\infty} w(y, x - y) e^{-0.01x} x^{-0.99} dx \right) e^{0.136193(u-y)} dy, \quad u > b. \end{aligned} \tag{52}$$

For the asymptotics of $m(u), u > b$, we test the following three cases:

(1) Choose $w(x, y) \equiv 1$. For this case, it follows from (41) that

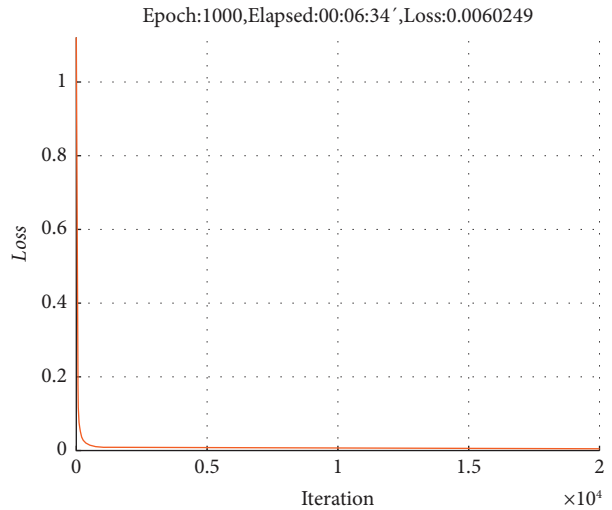

Figure 4: Variation of the loss function.

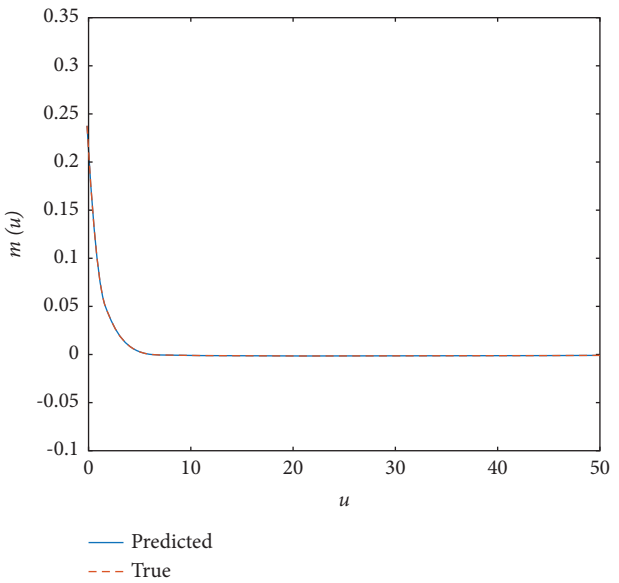

Figure 5: Comparison of the exact and numerical solutions.

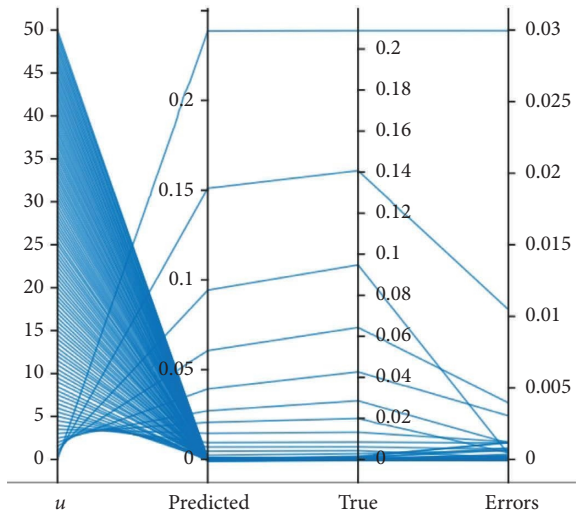

Figure 6: Errors of the numerical solution.

Table 1: Errors of the numerical solution.

u	Predicted	True	Errors
0.0000	0.2392	0.2092	0.0300
1.0000	0.0945	0.0949	0.0004
2.0000	0.0399	0.0430	0.0031
3.0000	0.0199	0.0195	0.0004
4.0000	0.0100	0.0088	0.0012
5.0000	0.0041	0.0040	0.0001
6.0000	0.0006	0.0018	0.0012
7.0000	0.0000	0.0008	0.0008
8.0000	0.0000	0.0004	0.0004
9.0000	0.0000	0.0002	0.0002
10.0000	0.0000	0.0001	0.0001
11.0000	0.0000	0.0000	0.0000
12.0000	0.0000	0.0000	0.0000

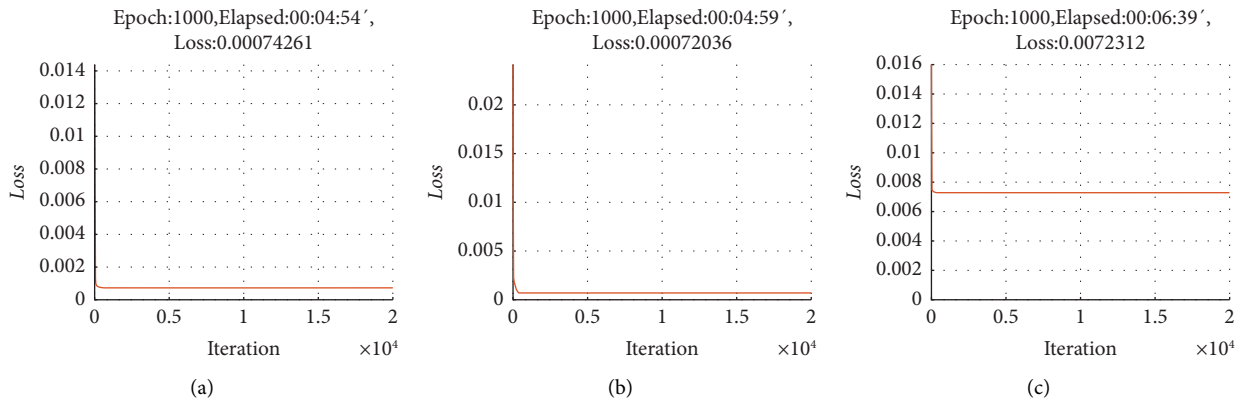

Figure 7: Variation of the loss function *Loss* with different penalties at ruin ((a) $w(x,y) \equiv 1$, (b) $w(x,y) = e^{0.01x}$, and (c) $w(x,y) = (1 - e^{1-y}) \vee 0$).

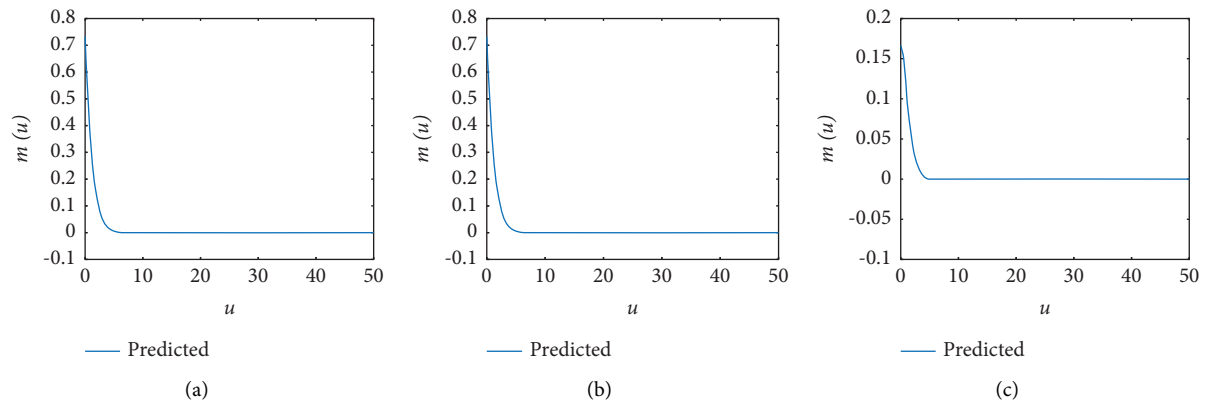

Figure 8: Numerical solution of $m(u)$ with different penalties at ruin ((a) $w(x,y) \equiv 1$, (b) $w(x,y) = e^{0.01x}$, and (c) $w(x,y) = (1 - e^{1-y}) \vee 0$).

$$m(u) \sim 0.00112992e^{-0.00999827u}. \tag{53}$$

(2) Choose $w(x,y) = e^{0.0001x}$. For this case, it follows from (41) that

$$m(u) \sim 0.0455311e^{-0.00999827u}. \tag{54}$$

(3) Choose $w(x,y) = (1 - e^{1-y}) \vee 0$, For this case, it follows from (41) that

Table 2: Numerical results of asymptotics of $m(u)$.

u	Asymptotics for case 1	Asymptotics for case 2	Asymptotics for case 3
10	0.001022412	0.041198956	0.000995239
20	0.000925132	0.037279002	0.000900545
30	0.000837109	0.033732019	0.000814861
40	0.000757460	0.030522521	0.000737329
50	0.000685390	0.027618397	0.000667175
60	0.000620178	0.024990591	0.000603695
70	0.000561170	0.022612813	0.000546255
80	0.000507776	0.020461273	0.000494281
90	0.000459463	0.018514446	0.000447252
100	0.000415746	0.016752854	0.000404697

$$m(u) \sim 0.00109989e^{-0.00999827u}. \tag{55}$$

We take advantage of the package Mathematica 12.0 to examine the asymptotic formula (41). The numerical results of asymptotics of $m(u)$ are copied to Table 2.

5. Conclusion

In this paper, we derive an integrodifferential equation and a defective renewal equation for the expected discounted penalty function with threshold dividend strategy and stochastic discount rate and then find the solutions of the equations. We creatively propose the PINN method for finding the numerical solution of the integrodifferential equation. Given initial and boundary conditions, this method allows finding the numerical results of the expected discounted penalty function quickly. The example in this paper demonstrates the effectiveness of the PINN method in which the numerical solution is very close to the exact solution. We hope to apply this method to find numerical solutions of the expected discounted penalty function where the individual claim amount distribution is arbitrary in the future.

Data Availability

The data used to support this study are included within the article.

Additional Points

Use of AI Tools Declaration. The authors declare they have not used Artificial Intelligence (AI) tools in the creation of this article.

Conflicts of Interest

The authors declare that there are no conflicts of interest regarding the publication of this paper.

Acknowledgments

This research was supported by the Natural Science Research Project of Anhui Jianzhu University (Grant no. KJ0514).

References

[1] H. U. Gerber and E. S. W. Shiu, "On the time value of ruin," *North American Actuarial Journal*, vol. 2, no. 1, pp. 48–72, 1998.

[2] A. E. Kyprianou, "The Gerber–Shiu measure," in *Gerber–Shiu Risk Theory*, pp. 37–44, Springer International Publishing Company Limited, Cham, Switzerland, 2013.

[3] G. E. Willmot and J. K. Woo, "Gerber–Shiu analysis in the dependent Sparre Andersen model," in *Surplus Analysis of Sparre Andersen Insurance Risk Processes*, pp. 61–78, Springer International Publishing Company Limited, Cham, Switzerland, 2017.

[4] X. Sheldon Lin, G. E Willmot, and S. Drekic, "The classical risk model with a constant dividend barrier: analysis of the Gerber–Shiu discounted penalty function," *Insurance: Mathematics and Economics*, vol. 33, no. 3, pp. 551–566, 2003.

[5] L. Ramsden and A. D. Papaioannou, "Asymptotic results for a Markov–modulated risk process with stochastic investment," *Journal of Computational and Applied Mathematics*, vol. 313, pp. 38–53, 2017.

[6] R. Loeffen, Z. Palmowski, and B. A. Surya, "Discounted penalty function at Parisian ruin for Lévy insurance risk process," *Insurance: Mathematics and Economics*, vol. 83, pp. 190–197, 2018.

[7] M. Preischl and S. Thonhauser, "Optimal reinsurance for Gerber–Shiu functions in the Cramér–Lundberg model," *Insurance: Mathematics and Economics*, vol. 87, pp. 82–91, 2019.

[8] E. M. Martín–González and E. T. Kolkovska, "Expected discounted penalty function and asymptotic dependence of the severity of ruin and surplus prior to ruin for two–sided Lévy risk processes," *Communications in Statistics- Theory and Methods*, vol. 52, no. 23, pp. 8566–8583, 2023.

[9] Y. He, R. Kawai, Y. Shimizu, and K. Yamazaki, "The Gerber–Shiu discounted penalty function: a review from practical perspectives," *Insurance: Mathematics and Economics*, vol. 109, pp. 1–28, 2023.

[10] E. M. Martín–González, A. Murillo-Salas, and H. Pantí, "Gerber–Shiu function for a class of Markov–modulated Lévy risk processes with two–sided jumps," *Methodology and Computing in Applied Probability*, vol. 24, no. 4, pp. 2779–2800, 2022.

[11] Z. Zhou, H. Xiao, and Y. Deng, "Markov–dependent risk model with multi-layer dividend strategy," *Applied Mathematics and Computation*, vol. 252, pp. 273–286, 2015.

[12] O. Ragulina, "The risk model with stochastic premiums and a multi–layer dividend strategy," *Modern Stochastics: Theory and Applications*, vol. 6, no. 3, pp. 285–309, 2019.

[13] T. Zhou, X. Liu, M. Hou, and C. Liu, "Numerical solution for ruin probability of continuous time model based on neural network algorithm," *Neurocomputing*, vol. 331, pp. 67–76, 2019.

[14] M. Ma, L. Zheng, and J. Yang, "A novel improved trigonometric neural network algorithm for solving price-dividend functions of continuous time one-dimensional asset–pricing models," *Neurocomputing*, vol. 435, pp. 151–161, 2021.

[15] M. Ma, J. Yang, and R. Liu, "A novel structure automatic-determined Fourier extreme learning machine for generalized Black–Scholes partial differential equation," *Knowledge-Based Systems*, vol. 238, Article ID 107904, 2022.

[16] M. Raissi, P. Perdikaris, and G. E. Karniadakis, "Physics-informed neural networks: a deep learning framework for solving forward and inverse problems involving nonlinear partial differential equations," *Journal of Computational Physics*, vol. 378, pp. 686–707, 2019.

[17] A. G. Baydin, B. A. Pearlmutter, A. A. Radul, and J. M. Siskind, "Automatic differentiation in machine learning: a survey," *Journal of Machine Learning Research*, vol. 18, no. 153, pp. 1–43, 2018.

[18] G. Tzougas and K. Kutzkov, "Enhancing logistic regression using neural networks for classification in actuarial learning," *Algorithms*, vol. 16, no. 2, Article ID 16020099, 2023.

[19] G. Wu, F. Wang, and L. Qiu, "Physics-informed neural network for solving the Hausdorff derivative Poisson equations," *Fractals*, vol. 31, no. 06, Article ID 2340103, 2023.

[20] B. Zhang, G. Wu, Y. Gu, X. Wang, and F. Wang, "Multi–domain physics–informed neural network for solving forward and inverse problems of steady–state heat conduction in multilayer media," *Physics of Fluids*, vol. 34, no. 11, Article ID 116116, 2022.

[21] B. Zhang, F. Wang, and L. Qiu, "Multi–domain physics–informed neural networks for solving transient heat conduction problems in multilayer materials," *Journal of Applied Physics*, vol. 133, no. 24, Article ID 245103, 2023.

[22] Y. Ma, X. Xu, S. Yan, and Z. Ren, "A preliminary study on the resolution of electro–thermal multi–physics coupling problem using physics–informed neural network (PINN)," *Algorithms*, vol. 15, no. 2, Article ID 15020053, 2022.

[23] S. Asmussen and H. Albrecher, "The compound Poisson model," in *Ruin Probabilities*, pp. 57–96, World Scientific Publishing Company Limited, Singapore, 2nd edition, 2010.

[24] J. Grandell, "The classical risk model," in *Aspects of Risk Theory*, pp. 1–32, Springer-Verlag, New York, NY, USA, 1991.

[25] X. S. Lin and K. P. Pavlova, "The compound Poisson risk model with a threshold dividend strategy," *Insurance: Mathematics and Economics*, vol. 38, no. 1, pp. 57–80, 2006.

[26] H. Zhang, M. Zhou, and J. Guo, "The Gerber–Shiu discounted penalty function for classical risk model with a two-step premium rate," *Statistics and Probability Letters*, vol. 76, no. 12, pp. 1211–1218, 2006.

[27] N. Privault, "Forward rate modeling," in *An Elementary Introduction to Stochastic Interest Rate Modeling*, World Scientific Publishing Company Limited, Singapore, 2012.

[28] H. Wang and N. Ling, "On the Gerber-Shiu function with random discount rate," *Communications in Statistics- Theory and Methods*, vol. 46, no. 1, pp. 210–220, 2017.

[29] W. Wang, P. Chen, and S. Li, "Generalized expected discounted penalty function at general drawdown for Lévy risk processes," *Insurance: Mathematics and Economics*, vol. 91, pp. 12–25, 2020.

[30] X. Li, Y. Shi, S. C. Phillip Yam, and H. Yang, "Fourier–cosine method for finite-time Gerber–Shiu functions," *SIAM Journal on Scientific Computing*, vol. 43, no. 3, pp. 650–677, 2021.

[31] D. C. M. Dickson, "Some explicit solutions for the joint density of the time of ruin and the deficit at ruin," *ASTIN Bulletin*, vol. 38, no. 1, pp. 259–276, 2008.